

## Article

# Effect of TiO<sub>2</sub> on Thermal, Mechanical, and Gas Separation Performances of Polyetherimide–Polyvinyl Acetate Blend Membranes

Khuram Maqsood <sup>1,\*</sup>, Asif Jamil <sup>2</sup> , Anas Ahmed <sup>3</sup>, Burhannudin Sutisna <sup>4</sup> , Suzana Nunes <sup>5</sup> and Mathias Ulbricht <sup>6</sup>

<sup>1</sup> Department of Chemical Engineering, University of Jeddah, Jeddah 23890, Saudi Arabia

<sup>2</sup> Department of Chemical, Polymer and Composite Materials Engineering, University of Engineering and Technology (New Campus), Lahore 39021, Pakistan

<sup>3</sup> Department of Industrial and System Engineering, University of Jeddah, Jeddah 23890, Saudi Arabia

<sup>4</sup> Department of Food Engineering, Faculty of Industrial Technology, Bandung Institute of Technology, Jalan Let. Jen. Purn. Dr. (HC). Mashudi No.1, Sumedang 45363, Indonesia

<sup>5</sup> Biological and Environmental Science and Engineering Division (BESE), King Abdullah University of Science and Technology (KAUST), Thuwal 23955-6900, Saudi Arabia

<sup>6</sup> Lehrstuhl für Technische Chemie II, Universität Duisburg-Essen, 45117 Essen, Germany

\* Correspondence: kmaqsood@uj.edu.sa

**Abstract:** Blend membranes consisting of two polymer pairs improve gas separation, but compromise mechanical and thermal properties. To address this, incorporating titanium dioxide (TiO<sub>2</sub>) nanoparticles has been suggested, to enhance interactions between polymer phases. Therefore, the objective of this study was to investigate the impact of TiO<sub>2</sub> as a filler on the thermal, surface mechanical, as well as gas separation properties of blend membranes. Blend polymeric membranes consisting of polyetherimide (PEI) and polyvinyl acetate (PVAc) with blend ratios of (99:1) and (98:2) were developed via a wet-phase inversion technique. In the latter, TiO<sub>2</sub> was incorporated in ratios of 1 and 2 wt.% while maintaining a blend ratio of (98:2). TGA and DSC analyses were used to examine thermal properties, and nano-indentation tests were carried out to ascertain surface mechanical characteristics. On the other hand, a gas permeation set-up was used to determine gas separation performance. TGA tests showed that blend membranes containing TiO<sub>2</sub> had better thermal characteristics. Indentation tests showed that TiO<sub>2</sub>-containing membranes exhibited greater surface hardness compared to other membranes. The results of gas permeation experiments showed that TiO<sub>2</sub>-containing membranes had better separation characteristics. PEI–PVAc blend membranes with 2 wt.% TiO<sub>2</sub> as filler displayed superior separation performance for both gas pairs (CO<sub>2</sub>/CH<sub>4</sub> and CO<sub>2</sub>/N<sub>2</sub>). The compatibility between the rubbery and glassy phases of blend membranes was improved as a result of the inclusion of TiO<sub>2</sub>, which further benefited their thermal, surface mechanical, and gas separation performances.

**Keywords:** polyetherimide; polyvinyl acetate; titanium dioxide; blend membrane; composite membrane; gas separation



**Citation:** Maqsood, K.; Jamil, A.; Ahmed, A.; Sutisna, B.; Nunes, S.; Ulbricht, M. Effect of TiO<sub>2</sub> on Thermal, Mechanical, and Gas Separation Performances of Polyetherimide–Polyvinyl Acetate Blend Membranes. *Membranes* **2023**, *13*, 734. <https://doi.org/10.3390/membranes13080734>

Academic Editor: Klaus Rätzke

Received: 8 July 2023

Revised: 27 July 2023

Accepted: 10 August 2023

Published: 15 August 2023



**Copyright:** © 2023 by the authors. Licensee MDPI, Basel, Switzerland. This article is an open access article distributed under the terms and conditions of the Creative Commons Attribution (CC BY) license (<https://creativecommons.org/licenses/by/4.0/>).

## 1. Introduction

Membrane technology resulting in benefits in terms of energy efficiency and from an economical point of view is regarded as a viable emerging technology in gas separation applications [1,2]. Nevertheless, due to the inherent trade-off between gas permeability and selectivity, commercially available membranes (either organic or inorganic) used in gas separation are available with particular constraints [3,4]. A probable and viable alternative in membrane-based gas separation technology is the use of polymer blends. However, one of the main challenges of this approach is establishing compatibility between paired

polymers while maintaining the desired mechanical properties. Blending different polymers together can create composite materials that synergistically combine the properties of the individual components, which would otherwise be unattainable [5]. Adjusting the composition can obtain customized properties for specific applications. In particular, for membrane-based gas separations, it is advantageous to have a dense structure that facilitates the solution–diffusion mechanism. Therefore, in addition to considering the sizes of gases that pass through the membrane, it is also crucial to take into account the interaction between the molecules and the membrane.

Previous studies of polymer blends have highlighted the issue of immiscibility, which affects the physical and chemical properties of the product at the molecular level. Although immiscible blends are commercially available, their propensity to exhibit unstable phase morphology during melt processing frequently leads to inadequate mechanical performance [6,7]. To achieve a fine and stable morphology and improve the properties of the blend, the use of a suitable compatibilizer that acts as a surfactant has been explored [8]. This compatibilizer facilitates better interfacial interactions of the polymer phases and enhances the properties of the blend [8,9]. The most commonly used compatibilizer is a copolymer derived from monomers of the matrix polymer that is present in the blend. However, the complex synthesis process and limited applicability of specific blends have led researchers to seek better alternatives [10]. Recently, there has been a significant increase in studying the incorporation of nanoparticles into immiscible polymer blends. The nano-effects of these nanoparticles not only reduce phase separation behavior in the blend, but also enhance the mechanical and thermal stabilities of the resulting blend membrane [11]. Based on this hypothesis, incorporating nanoparticles into a PEI–PVAc blend can improve the physiochemical properties of the blend and enhance compatibility by refining the co-continuous structure of the blend through the addition of TiO<sub>2</sub> nano-particles.

Based on these observations as a reference point, this study aimed to investigate the impact of incorporating TiO<sub>2</sub> into a PEI–PVAc blend membrane on its thermal, surface mechanical, and gas separation properties. The blending of a glassy and a rubbery polymer was intended to enhance the performance of the membrane systems by leveraging the distinctive gas separation characteristics of the parent polymers, while also introducing additional binding sites for carbon dioxide (CO<sub>2</sub>) at the molecular level. In the realm of membrane enhancement for gas separation, there are various additives, such as carbon black, carbon nanotubes, silica, nano-clay, and titanium oxide [12]. The structure of titanium dioxide is depicted in Figure 1. Li et al. reported improved mechanical stability in polymer membranes through the incorporation of TiO<sub>2</sub> nanoparticles [13]. They also found that the addition of TiO<sub>2</sub> reduced the solvent's precipitation rate during membrane formation, leading to a denser skin layer in the cross-section of the membrane. Furthermore, with the addition of TiO<sub>2</sub> nanoparticles, Madaeni et al. observed a corresponding rise in membrane wall thickness, as well as improved separation properties [14]. In a separate investigation, Ahmad et al. successfully prepared PVAc membranes incorporated with TiO<sub>2</sub> nanocomposites, resulting in improved thermal stability and enhanced membrane performance [15]. Similarly, Cai et al. observed a reduction in the co-continuous phase of a polystyrene–polyamide (PS–PA6) blend upon the addition of TiO<sub>2</sub> [16]. Hu et al. developed a poly(amide-imide)–TiO<sub>2</sub> nanocomposite membrane that exhibited superior gas separation performance compared to pure poly(amide-imide), even at low TiO<sub>2</sub> loading [17].

Based on these findings, this study hypothesized that incorporating inorganic moieties into the blend system would improve developed membranes' mechanical and thermal characteristics. TiO<sub>2</sub> was chosen as a key parameter for investigating the effects of incorporating these nanoparticles into the polymer blend, with the aim to improve the thermal and surface properties of blend membranes. Additionally, the gas separation performances of the membranes were analyzed by varying composition, temperature, and gas pressure.

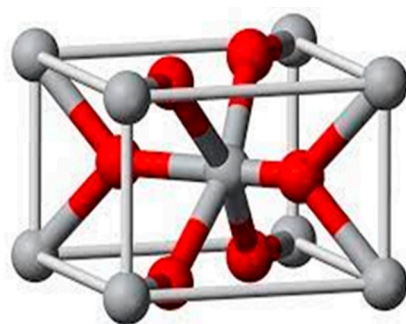


**Figure 1.** Structure of titanium dioxide.

## 2. Experimental

### 2.1. Materials

Prior to use, PEI pellets (with a melt flow index of approximately 9 g/10 min) were dehydrated in a 100 °C oven for 24 h to remove any moisture content. Conversely, PVAc beads (with a density of approximately 1.19 g/cm<sup>3</sup> at 25 °C) were used as received without undergoing prior drying. An organic solvent, *N*-methyl-2-pyrrolidone (NMP), with a purity of 99.5%, was employed. In addition, particulate fillers were incorporated, consisting of TiO<sub>2</sub> nanoparticles with a primary particle size of 21 nm. All the aforementioned chemicals were obtained from Sigma Aldrich (St. Louis, MO, USA).

### 2.2. Methods

In this study, different membranes, including pure PEI, PEI–PVAc blends, and PEI–PVAc blends with TiO<sub>2</sub> nanoparticles, were prepared. Based on the optimized polymeric membrane ratio observed through previous investigations, the PEI–PVAc polymer blend's ratio was established at (98:2) [18]. The pure and blend polymeric dope solutions were prepared following the methods outlined in our previous study.

However, for the PEI–PVAc–TiO<sub>2</sub> membrane, a different approach was taken. In order to ensure homogeneity, TiO<sub>2</sub> nanoparticles were first dispersed in NMP and stirred for 30 min. TiO<sub>2</sub> particles were then subjected to an additional 30 min of ultrasonication in order to efficiently disperse them within the solvent. In a separate process, one half of the PEI was dissolved in NMP over the course of three hours at a temperature of 70 °C. Subsequently, to ensure complete dissolution, the rest of the PEI pellets and PVAc polymers were gradually added to the solution, while raising the temperature to 90 °C for a duration of nine hours. After the preparation of the solution, degassing procedures were conducted for a period of 12 h under ambient conditions to eliminate any trapped air bubbles.

### 2.3. Membrane Fabrication

The membrane casting solution was applied onto a glass plate and uniformly spread using a casting knife by adjusting the film thickness to 150 µm. When the casting process was completed, the freshly formed membranes were placed in a bath of room temperature water. The membranes were then submerged in distilled water for three days, followed by air-drying at room temperature to ensure the complete removal of any remaining solvent. Table 1 provides the developed membranes and their respective properties.

**Table 1.** Compositions of developed membranes and their respective glass transition temperatures (T<sub>g</sub>).

Membrane Code	PEI (wt.%)	PVAc (wt.%)	TiO <sub>2</sub> (wt.%)	T <sub>g</sub> (°C)
PEI	100	-	-	212
PP(1)	99	1	-	211
PP(2)	98	2	-	209
PPT(1)	98	2	1	210
PPT(2)	98	2	2	212

The phase inversion method was adopted; as a result, the developed membrane was asymmetric, with a dense layer at the top and finger-like pores beneath, as depicted in Figure 2.

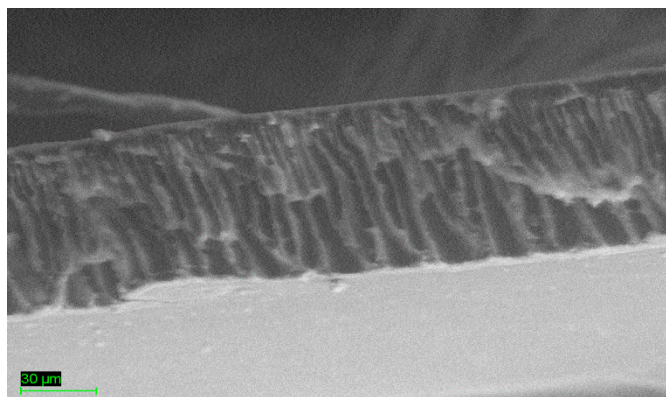


**Figure 2.** Cross-sectional view of the PEI–PVAc blend membrane.

#### 2.4. Characterization and Gas Permeation Tests of the Developed Membranes

##### 2.4.1. Thermal Analysis of the Membranes

Using a TGA (thermogravimetric analysis) analyzer (Perkin Elmer, Waltham, MA, USA, STA6000) in a nitrogen atmosphere, the blend membranes' thermal characteristics were assessed. The measurements were carried out in the 30 to 600 °C temperature range with the heating rate set at 10 °C/min. The glass transition temperatures ( $T_g$ ) of the cast membranes were determined using DSC (differential scanning calorimetry) analysis. The membrane samples were heated in a nitrogen atmosphere from room temperature to 250 °C, and then returned to room temperature at a rate of 10 °C/min.

##### 2.4.2. Nano-Indentation Technique

Indentation tests were performed using the continuous stiffness measurement technique, which involves monitoring and recording the dynamic load and indenter of a diamond tip using the three-sided pyramid geometry displacement of a three-sided pyramidal diamond (Berkovich) indenter, as depicted in Figure 3a. The indenter had a tip radius of 0.219 μm with an effective tip-opening angle of 140.6°. This test was carried out in load-controlled mode, with the indentation load maintained at approximately 100 mN. At least 9 points were indented on each membrane; the specific indentation points for the pure PEI membrane sample are depicted in Figure 3b. Nanoindentation provided a means to measure mechanical properties of thin layers.

##### 2.4.3. Gas Permeation Study of the Developed Membranes

Permeability testing for pure CO<sub>2</sub>, N<sub>2</sub>, and CH<sub>4</sub> gases was performed on developed membranes using a gas permeation unit specifically designed for these measurements. During testing, the gas pressure and permeation testing temperature were varied. To ensure accurate measurements, any remaining gases in the device were expelled using a vacuum pump prior to testing to ensure precise measurements. Maintaining atmospheric pressure kept the pressure on the permeate side of the membrane constant. The permeation rates of gas streams were measured using a bubble flow-meter capable of detecting flow rates as low as 100 mL/min. The following equation was used to calculate the gas permeation:

$$\frac{P_x}{l} = \frac{Q}{A\Delta P} \frac{273.15}{T} \quad (1)$$

$$\alpha_{xy} = \frac{P_x}{P_y} \quad (2)$$

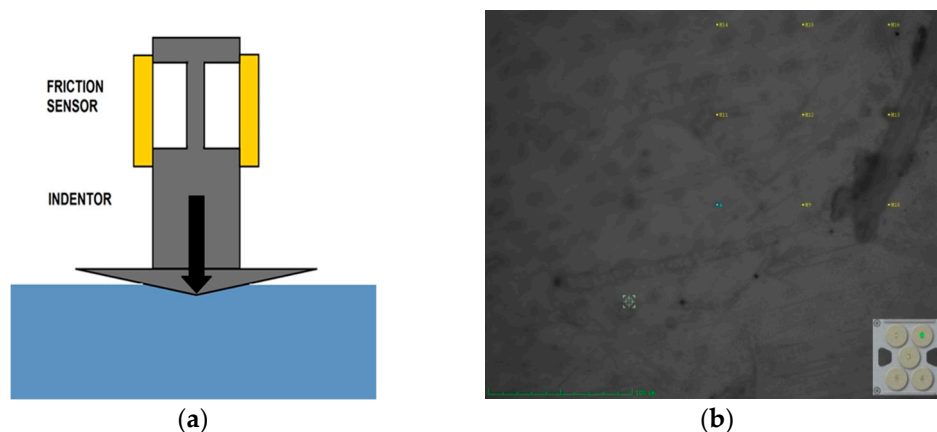


**Figure 3.** Schematic diagram of (a) indenter on the surface and (b) PEI membrane surface and indentation points.

The GPU measurement unit is used to quantify gas permeance ( $P_x/l$ ), where 'x' denotes the gas being studied ( $N_2$ ,  $CO_2$ , or  $CH_4$ ). The volumetric flow rate is represented by 'Q', and the effective surface area of the membrane is denoted by 'A'. The permeation process occurs at a specific temperature ( $T$ ) and is conducted by applying a pressure difference ( $\Delta P$ ). The ideal selectivity, denoted as  $\alpha_{xy}$ , represents the ratio of the permeabilities of the competing incident gases x and y across the membrane.

### 3. Results and Discussion

#### 3.1. Thermal Analysis

The thermal properties of the developed membranes were assessed through TGA and DSC analysis. Decomposition curves (Figure 4) indicated a single major mass loss for all membrane fibers. Notably, no weight loss was observed below 100 °C, indicating the absence of moisture in the developed membranes. The pure PEI membrane exhibited an onset temperature of approximately 440 °C, consistent with the previously published literature [19]. A 10% weight loss was used as a reference point to compare the degradation of the membranes. Weight loss between 100 and 300 °C is referred to as the mass of solvent retained in the membranes that evaporated as the temperature increased.

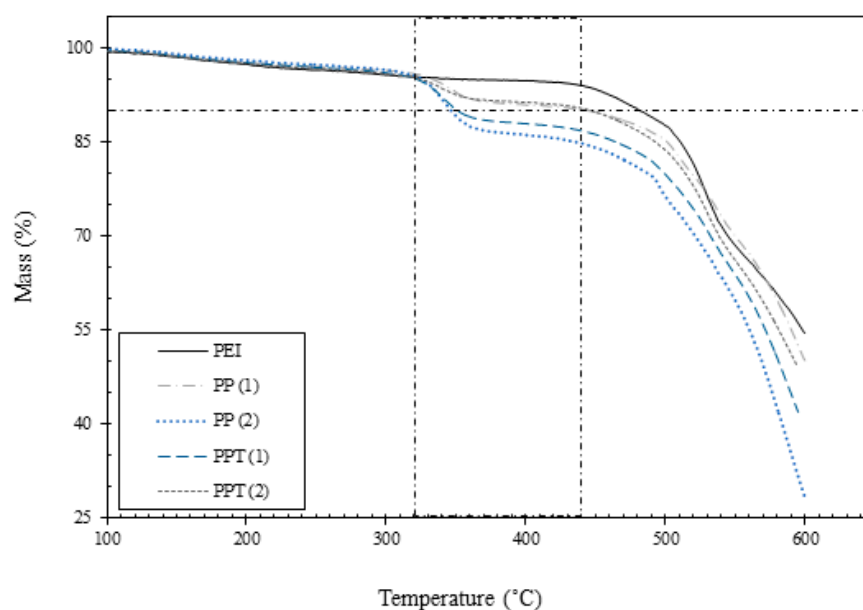


**Figure 4.** TGA analysis of developed membranes.



Furthermore, it was observed that the addition of PVAc to the PEI matrix resulted in a decrease in thermal properties as the proportion of the rubbery phase increased. In reference to the degradation temperature, neat PEI displayed a degradation temperature of 482 °C, which decreased to 340 °C for PP(2). These findings imply that adding rubbery PVAc to the glassy PEI matrix reduces its thermal properties. However, this trend was reversed with the addition of TiO<sub>2</sub> into the blend membranes. The incorporation of 2 wt.% of TiO<sub>2</sub> into the PEI–PVAc blend led to a recovery in the degradation temperature, which reached 450 °C. This indicates that an improvement in thermal stability was achieved by adding titanium to the blend membrane. Similar observations have been reported, such as the development of a polyethersulfone (PES) and PVAc blend membrane, which exhibited lower thermal stability compared to a plain PES membrane [20]. However, the addition of TiO<sub>2</sub> reversed the thermal stability and restored it. These observations have also been reported in other studies [21].

The stiffness of polymeric materials is characterized by their  $T_g$  values, which were determined through DSC analysis, and are shown in Table 1. It can be observed that the  $T_g$  of pure PEI was approximately 212 °C, which aligns with the previous literature [18]. As the proportion of the rubbery PVAc component increased in the blend, the flexibility of the structure also increased, resulting in a lower  $T_g$ , as indicated in Table 1. However, the presence of a single  $T_g$  value suggests a uniform blending of the two polymers in the blend samples.

Nevertheless, the introduction of TiO<sub>2</sub> resulted in a distinct and singular  $T_g$  value across all tested membranes, indicating a molecular-level combination of polymer chains and TiO<sub>2</sub>, and the formation of a new material. The TiO<sub>2</sub> content of blend membranes caused the  $T_g$  value to increase. The homogeneous dispersion of titanium nanoparticles, which combined with the polymeric chains and decreased the free volume within the polymer structure, was responsible for this increase. Consequently, this restriction in the movement of chain fragments caused the polymer chains to become more rigid and raised the  $T_g$  value. Numerous authors have extensively documented the rise of  $T_g$  with the incorporation of TiO<sub>2</sub> into the polymer matrix in the literature [22].

### 3.2. Surface Mechanical Analysis

Figure 5 illustrates the compliance curve of neat PEI, PP(2), and PPT(2) membranes. A total of nine indents were applied to each sample, with a spacing of 40 µm between them. The membrane samples were subjected to a constant load of 15 mN, resulting in a maximum penetration depth of 15 µm. The unloading phase following the application of constant force exhibited a creep region, as depicted in Figure 5. Creep refers to a change in depth over time while maintaining a constant force, and it reached a new limit just before unloading. Subsequently, the indenter began to unload. The absence of overlap between the loading and unloading curves shown in Figure 5 suggests that the developed membranes demonstrated both elastic behavior and distinct plastic characteristics [23]. The loading and unloading curves appeared continuous and stable for all developed membranes.

The spacing between indents was adjusted to prevent overlapping of the internal stress generated around each indent. In the case of the neat PEI sample, the indenter penetrated up to a maximum contact depth of 7.7 µm, while this value increased to 14.00 µm for PP(2). However, the value decreased to 5.08 µm for the blend sample incorporating 2 wt.% of TiO<sub>2</sub>. It can be observed that the presence of PVAc in the PEI matrix reduced the hardness and stiffness of the surface. Conversely, incorporating TiO<sub>2</sub> nanoparticles into the blend sample caused the surface to become stiff and hard. This can be attributed to the uniform dispersion of TiO<sub>2</sub> nanoparticles within the polymer matrix, which imparted stiffness to the membranes. These findings are indirectly validated by the thermal analysis discussed in the previous section. Consistent with the previous literature, the addition of nanoparticles inside the polymer matrix resulted in a stiffer and harder surface [24]. Therefore, appropriate dispersion of nanoparticles can enhance membrane hardness and resistance to indenter penetration.

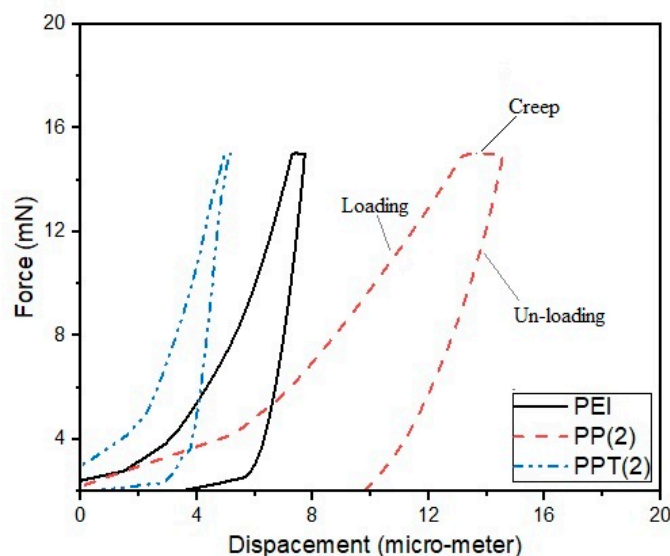


**Figure 5.** Load displacement analysis of casted membranes.

### 3.3. Gas Permeation Study

Figure 6 depicts the  $\text{CO}_2$  permeance and ideal selectivity ( $\text{CO}_2/\text{CH}_4$ ,  $\text{CO}_2/\text{N}_2$ ) of pure PEI, PEI-PVAc blend, and PES-PVAc-TiO<sub>2</sub> membranes. The figure clearly demonstrates that the composite membrane outperformed the other membranes in terms of performance.  $\text{CO}_2$  permeance showed an increasing trend with the addition of PVAc. The permeance of  $\text{CO}_2$  in the PEI-PVAc (98:2) blend membrane was 26.1% higher than that of the neat PEI membrane at ambient temperature and 2 bar pressure. The inclusion of the rubbery PVAc phase in the blend led to polymer chains being loosely packed, resulting in increased free volume. This loose structure facilitated the diffusion of smaller molecules through the blend matrix. As a result, the addition of the rubbery PVAc component enhanced the permeation of  $\text{CO}_2$ ,  $\text{CH}_4$ , and  $\text{N}_2$ . Furthermore, the  $\text{CO}_2$  benefited from higher solubility and a smaller kinetic diameter, which gave it an advantage in dissolving and diffusing through the blend membrane matrix. This advantage was reflected in the relative ideal selectivity of the developed blend membrane. Similar observations were reported by Farman et al. when PVAc was added to PES [25]. They observed (compared to neat PES) an almost double value of  $\text{CO}_2$  permeance and a 3.6 times increase in ideal ( $\text{CO}_2/\text{CH}_4$ ) selectivity at 10 bar pressure.

On the other hand, the incorporation of TiO<sub>2</sub> also had a positive impact on the  $\text{CO}_2$  permeance of the mixed matrix membrane. The  $\text{CO}_2$  permeance increased as the TiO<sub>2</sub> content in the blend increased. For a 2 wt.% addition of TiO<sub>2</sub> filler in the blend, the permeation was 36% higher compared to the neat sample. The incorporation of TiO<sub>2</sub> into the PES-PVAc polymer blend resulted in nanoparticle aggregation and the creation of voids at the TiO<sub>2</sub>-polymer interface, thereby enhancing gas diffusion through the membrane. Similar observations were reported by Abdullah et al. when TiO<sub>2</sub> nanoparticles were incorporated into PES-PVAc blend membranes [20]. They observed a 32.4% increase in  $\text{CO}_2$  permeance and a 65.9% surge in ideal ( $\text{CO}_2/\text{CH}_4$ ) selectivity at 10 bar pressure and 25 °C. Thus, the addition of TiO<sub>2</sub> nanoparticles proves advantageous for both gas selectivity and  $\text{CO}_2$  permeance in blend polymeric membranes. A similar behavior can be expected for  $\text{CO}_2/\text{N}_2$  selectivity, as the kinematic diameter of  $\text{N}_2$  gas molecules is also smaller compared to  $\text{CO}_2$ .

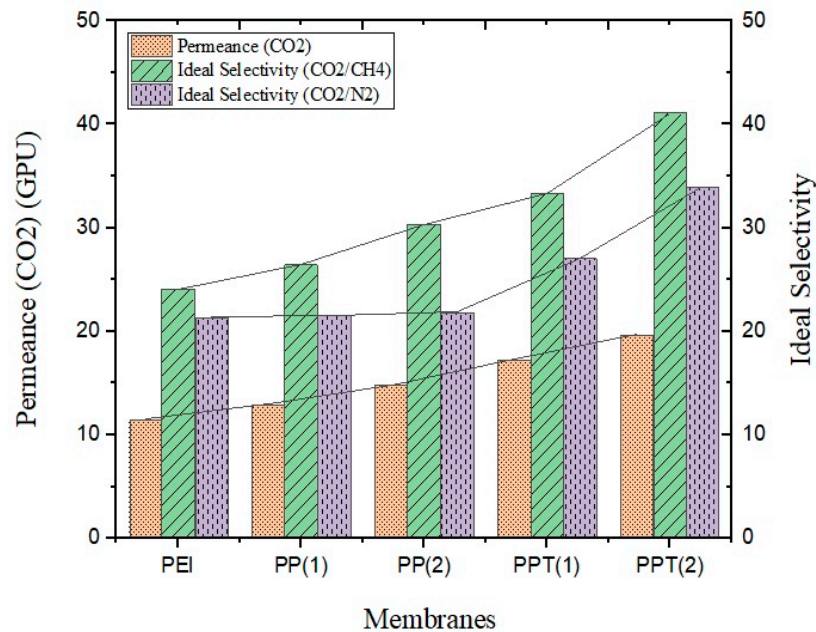


**Figure 6.** CO<sub>2</sub> permeance and ideal selectivity (CO<sub>2</sub>/CH<sub>4</sub>, CO<sub>2</sub>/N<sub>2</sub>) of developed membranes.

### 3.4. Effect of Feed Pressure

Gas permeation tests were conducted at different feed pressures and at room temperature for the best membranes prepared by adopting a PEI–PVAc blend (98:2) and 2 wt.% TiO<sub>2</sub> additions. Figure 7 depicts the gas permeations and ideal selectivity of the incident gases against the feed pressure; a noticeable trend can be observed wherein the permeance of CO<sub>2</sub> gas generally decreased as the feed pressure increased. The decline observed in this study aligns with earlier findings that indicated a decrease in gas permeability for polarizable gases (such as CO<sub>2</sub>) with increased pressure in glassy polymers. These findings further support the dual-mode sorption hypothesis [26]. Additionally, increased feed pressure caused the membrane matrix to contract, which lessened the effect of swelling. Together, these two elements lessen CO<sub>2</sub> permeability.

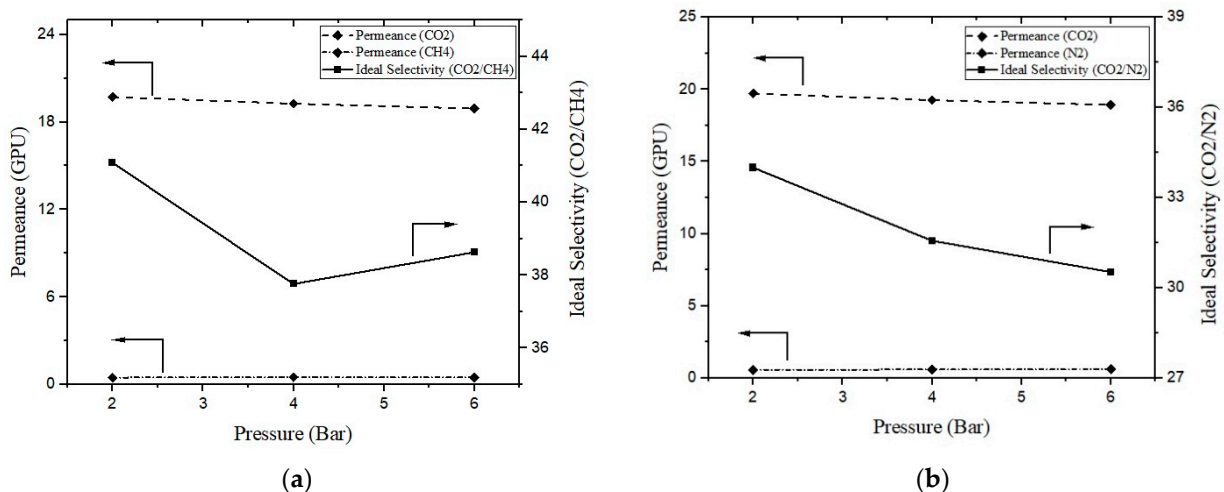


**Figure 7.** (a) CO<sub>2</sub> permeance and ideal selectivity (CO<sub>2</sub>/CH<sub>4</sub>) and (b) CO<sub>2</sub> permeance and (CO<sub>2</sub>/N<sub>2</sub>) selectivity of developed membranes against feed pressures.

Nonetheless, as the membrane swelling decreases, the competitive transport between CH<sub>4</sub>, N<sub>2</sub>, and CO<sub>2</sub> molecules is anticipated to become more pronounced. This phenomenon leads to a significant decline in gas selectivity. As depicted in Figure 7a,



the ideal selectivity for  $\text{CO}_2/\text{CH}_4$  gas decreased as the temperature increased. The value decreased from 41.1 to 38.6 as the temperature increased from 2 to 6 bar pressure. The effect of pressure change was more significant for  $\text{CO}_2/\text{N}_2$  gas, as the selectivity decreased from 34 to 30.53. These results are consistent with those reported in the literature [27]. In another study, Matsuyama et al. developed polyethylenimine (PEI)-poly(vinyl alcohol) (PVA) blend membranes, and observed that with an increase in feed pressure,  $\text{CO}_2$  permeance decreased and  $\text{N}_2$  permeance remained almost the same, thereby decreasing  $\text{CO}_2/\text{N}_2$  selectivity [28].

Therefore, it can be concluded that it is preferable to operate a prepared PPT(2) membrane at a relatively low feed pressure to attain a high separation performance for  $\text{CO}_2$  separation.

### 3.5. Effect of Temperature

For the most efficient PPT(2) membranes, gas permeation tests were carried out at different temperatures ranging from 25 to 45 °C and at 2 bar pressure. When the temperature increased from 25 to 45 °C, the  $\text{CO}_2$  permeance decreased significantly compared to other incident gases, such as  $\text{CH}_4$  and  $\text{N}_2$ , as the solubility of  $\text{CO}_2$  gas's polar nature is high compared to other gas molecules at room temperature. As the temperature increased, thermodynamically, the solubility of the  $\text{CO}_2$  gas significantly decreased compared to its counterparts, as depicted in Figure 8a,b. As the temperature increased, this declining trend in  $\text{CO}_2$  permeance had an impact on the developed membrane's ideal selectivity. The ideal selectivity for  $\text{CO}_2/\text{CH}_4$  over this temperature range decreased 25%. However, it was more prominent for  $\text{CO}_2/\text{N}_2$ , for which it reached 45%. These results suggest that these types of membranes are suitable at low to moderate temperatures. Khan et al. incorporated carbon nano sheets into a PEI matrix to develop composite membranes. The  $\text{CO}_2/\text{CH}_4$  ideal selectivity of the developed membranes was tested at various temperatures from 25 to 50 °C; a slight decreasing trend was observed [29].

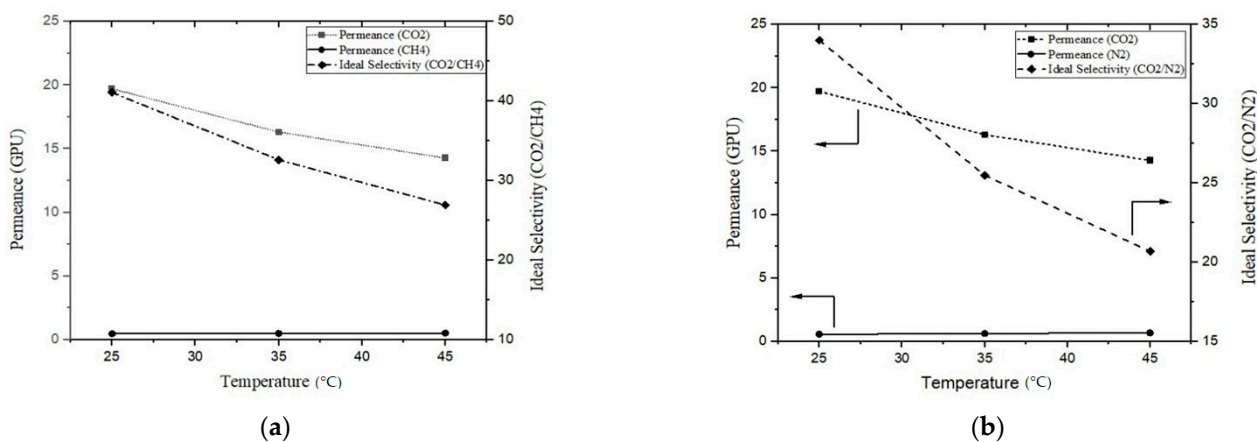


**Figure 8.** (a)  $\text{CO}_2$  permeance and ideal selectivity ( $\text{CO}_2/\text{CH}_4$ ) and (b)  $\text{CO}_2$  permeance and ( $\text{CO}_2/\text{N}_2$ ) selectivity of developed membranes against temperature.

## 4. Conclusions

This study investigated the impact of incorporating  $\text{TiO}_2$  nanoparticles into a PEI-PVAc blend membrane on its thermal, surface mechanical, and gas separation properties. Incorporating  $\text{TiO}_2$  nanoparticles into the blend membrane enhanced its thermal stability, as evidenced by TGA analysis. This improvement was reflected in a higher observed  $T_g$  value, as determined using DSC. Surface analysis revealed a stiffer and harder surface attributed to the uniform dispersion of nanoparticles within the polymer matrix compared to both neat and blend counterparts.

When compared to pure PEI, the PEI-PVAc blend membrane had better gas separation performance, and the addition of  $\text{TiO}_2$  nanoparticles improved ideal gas separation even

further. Optimal results were obtained with a 2 wt.% TiO<sub>2</sub> addition into the PEI–PVAc (98:2) matrix, achieving high selectivity for CO<sub>2</sub>/CH<sub>4</sub> and CO<sub>2</sub>/N<sub>2</sub>. These findings demonstrate the potential of incorporating nanoparticles to improve the performance of polymer blend membranes in gas separation applications.

**Author Contributions:** Conceptualization, K.M.; Methodology, A.J.; Formal analysis, B.S.; Investigation, A.J., A.A. and B.S.; Data curation, A.A.; Writing—original draft, K.M.; Writing—review & editing, S.N. and M.U.; Funding acquisition, K.M. All authors have read and agreed to the published version of the manuscript.

**Funding:** The research presented in this article was financially supported by the University of Jeddah, Jeddah, Saudi Arabia, under grant No. (UJ-21-ICI-14).

**Institutional Review Board Statement:** Not applicable.

**Data Availability Statement:** Not applicable.

**Acknowledgments:** The authors gratefully acknowledge the University of Jeddah’s technical and financial support.

**Conflicts of Interest:** The authors declare no conflict of interest.

## References

1. Jamil, A.; Ching, O.P.; Shariff, A.M. Polymer-nanoclay mixed matrix membranes for CO<sub>2</sub>/CH<sub>4</sub> separation: A review. *Appl. Mech. Mater.* **2014**, *625*, 690–695. [[CrossRef](#)]
2. Khurram, A.R.; Rafiq, S.; Tariq, A.; Jamil, A.; Iqbal, T.; Mahmood, H.; Mehdi, M.S.; Abdulrahman, A.; Ali, A.; Akhtar, M.S.; et al. Environmental remediation through various composite membranes moieties: Performances and thermomechanical properties. *Chemosphere* **2022**, *309*, 136613. [[CrossRef](#)] [[PubMed](#)]
3. Jansen, J.; Macchione, M.; Drioli, E. High flux asymmetric gas separation membranes of modified poly (ether ether ketone) prepared by the dry phase inversion technique. *J. Membr. Sci.* **2005**, *255*, 167–180. [[CrossRef](#)]
4. Buonomenna, M.G.; Figoli, A.; Jansen, J.C.; Drioli, E. Preparation of asymmetric PEEKWC flat membranes with different microstructures by wet phase inversion. *J. Appl. Polym. Sci.* **2004**, *92*, 576–591. [[CrossRef](#)]
5. Wong, K.K.; Jawad, Z.A. A review and future prospect of polymer blend mixed matrix membrane for CO<sub>2</sub> separation. *J. Polym. Res.* **2019**, *26*, 289. [[CrossRef](#)]
6. Panapitiya, N.P.; Wijenayake, S.N.; Huang, Y.; Bushdiecker, D.; Nguyen, D.; Ratanawanate, C.; Kalaw, G.J.; Gilpin, C.J.; Musselman, I.H.; Balkus, K.J.; et al. Stabilization of immiscible polymer blends using structure directing metal organic frameworks (MOFs). *Polymer* **2014**, *55*, 2028–2034. [[CrossRef](#)]
7. Kapantaidakis, G.; Kaldis, S.; Dabou, X.; Sakellaropoulos, G. Gas permeation through PSF-PI miscible blend membranes. *J. Membr. Sci.* **1996**, *110*, 239–247. [[CrossRef](#)]
8. Graziano, A.; Jaffer, S.; Sain, M. Review on modification strategies of polyethylene/polypropylene immiscible thermoplastic polymer blends for enhancing their mechanical behavior. *J. Elastomers Plast.* **2019**, *51*, 291–336. [[CrossRef](#)]
9. Chen, J.; Shi, Y.-Y.; Yang, J.-H.; Zhang, N.; Huang, T.; Wang, Y. Improving interfacial adhesion between immiscible polymers by carbon nanotubes. *Polymer* **2013**, *54*, 464–471. [[CrossRef](#)]
10. Wang, Y.; Zhang, Q.; Fu, Q. Compatibilization of immiscible poly (propylene)/polystyrene blends using clay. *Macromol. Rapid Commun.* **2003**, *24*, 231–235. [[CrossRef](#)]
11. Decol, M.; Pachekoski, W.M.; Becker, D. Compatibilization and ultraviolet blocking of PLA/PCL blends via interfacial localization of titanium dioxide nanoparticles. *J. Appl. Polym. Sci.* **2018**, *135*, 44849. [[CrossRef](#)]
12. Farrukh, S.; Javed, S.; Hussain, A.; Mujahid, M. Blending of TiO<sub>2</sub> nanoparticles with cellulose acetate polymer: To study the effect on morphology and gas permeation of blended membranes. *Asia-Pac. J. Chem. Eng.* **2014**, *9*, 543–551.
13. Li, J.-F.; Xu, Z.-L.; Yang, H.; Yu, L.-Y.; Liu, M. Effect of TiO<sub>2</sub> nanoparticles on the surface morphology and performance of microporous PES membrane. *Appl. Surf. Sci.* **2009**, *255*, 4725–4732. [[CrossRef](#)]
14. Madaeni, S.; Badieh, M.M.S.; Vatanpour, V.; Ghaemi, N. Effect of titanium dioxide nanoparticles on polydimethylsiloxane/polyethersulfone composite membranes for gas separation. *Polym. Eng. Sci.* **2012**, *52*, 2664–2674. [[CrossRef](#)]
15. Ahmad, J.; Deshmukh, K.; Hägg, M.B. Influence of TiO<sub>2</sub> on the chemical, mechanical, and gas separation properties of polyvinyl alcohol-titanium dioxide (PVA-TiO<sub>2</sub>) nanocomposite membranes. *Int. J. Polym. Anal. Charact.* **2013**, *18*, 287–296. [[CrossRef](#)]
16. Cai, X.; Li, B.; Pan, Y.; Wu, G. Morphology evolution of immiscible polymer blends as directed by nanoparticle self-agglomeration. *Polymer* **2012**, *53*, 259–266. [[CrossRef](#)]
17. Hu, Q.; Marand, E.; Dhingra, S.; Fritsch, D.; Wen, J.; Wilkes, G. Poly (amide-imide)/TiO<sub>2</sub> nano-composite gas separation membranes: Fabrication and characterization. *J. Membr. Sci.* **1997**, *135*, 65–79. [[CrossRef](#)]
18. Maqsood, K.; Jamil, A.; Ahmed, A.; Sutisna, B.; Nunes, S.; Ulbricht, M. Blend membranes comprising polyetherimide and polyvinyl acetate with improved methane enrichment performance. *Chemosphere* **2023**, *321*, 138074. [[CrossRef](#)]

19. Jamil, A.; Ching, O.P.; Shariff, A.M. Mixed matrix hollow fibre membrane comprising polyetherimide and modified montmorillonite with improved filler dispersion and CO<sub>2</sub>/CH<sub>4</sub> separation performance. *Appl. Clay Sci.* **2017**, *143*, 115–124. [[CrossRef](#)]
20. Abdullah, M.A.; Mukhtar, H.; Mannan, H.A.; Fong, Y.Y.; Shaharun, M.S. Polyethersulfone/polyvinyl acetate blend membrane incorporated with TiO<sub>2</sub> nanoparticles for CO<sub>2</sub>/CH<sub>4</sub> gas separation. *Malays. J. Fundam. Appl. Sci.* **2017**, *13*, 774–777. [[CrossRef](#)]
21. Azizi, N.; Mohammadi, T.; Behbahani, R.M. Synthesis of a new nanocomposite membrane (PEBAX-1074/PEG-400/TiO<sub>2</sub>) in order to separate CO<sub>2</sub> from CH<sub>4</sub>. *J. Nat. Gas Sci. Eng.* **2017**, *37*, 39–51. [[CrossRef](#)]
22. Ahmad, J.; Hågg, M.B. Polyvinyl acetate/titanium dioxide nanocomposite membranes for gas separation. *J. Membr. Sci.* **2013**, *445*, 200–210. [[CrossRef](#)]
23. Sulaiman, M.; Iqbal, T.; Yasin, S.; Mahmood, H.; Shakeel, A. Fabrication and Nanomechanical Characterization of Thermoplastic Biocomposites Based on Chemically Treated Lignocellulosic Biomass for Surface Engineering Applications. *Front. Mater.* **2021**, *8*, 408. [[CrossRef](#)]
24. Jamil, A.; Zulfiqar, M.; Arshad, U.; Mahmood, S.; Iqbal, T.; Rafiq, S.; Iqbal, M.Z. Development and performance evaluation of cellulose acetate-bentonite mixed matrix membranes for CO<sub>2</sub> separation. *Adv. Polym. Technol.* **2020**, *2020*, 8855577. [[CrossRef](#)]
25. Farnam, M.; Mukhtar, H.; Shariff, A.M. An investigation on polymeric blend mixed matrix membranes of polyethersulfone/polyvinyl acetate/carbon molecular sieve for CO<sub>2</sub>/CH<sub>4</sub> separation. *J. Fundam. Appl. Sci.* **2017**, *9*, 612–622.
26. Muruganandam, N.; Paul, D. Gas sorption and transport in miscible blends of tetramethyl bisphenol-A polycarbonate and polystyrene. *J. Polym. Sci. Part B Polym. Phys.* **1987**, *25*, 2315–2329. [[CrossRef](#)]
27. Li, Y.; Chen, D.; He, X. Preparation and Characterization of Polyvinylalcohol/Polysulfone Composite Membranes for Enhanced CO<sub>2</sub>/N<sub>2</sub> Separation. *Polymers* **2023**, *15*, 124. [[CrossRef](#)]
28. Matsuyama, H.; Terada, A.; Nakagawara, T.; Kitamura, Y.; Teramoto, M. Facilitated transport of CO<sub>2</sub> through polyethyleneimine/poly (vinyl alcohol) blend membrane. *J. Membr. Sci.* **1999**, *163*, 221–227. [[CrossRef](#)]
29. Khan, M.Y.; Khan, A.; Adewole, J.K.; Naim, M.; Basha, S.I.; Aziz, M.A. Biomass derived carboxylated carbon nanosheets blended polyetherimide membranes for enhanced CO<sub>2</sub>/CH<sub>4</sub> separation. *J. Nat. Gas Sci. Eng.* **2020**, *75*, 103156. [[CrossRef](#)]

**Disclaimer/Publisher's Note:** The statements, opinions and data contained in all publications are solely those of the individual author(s) and contributor(s) and not of MDPI and/or the editor(s). MDPI and/or the editor(s) disclaim responsibility for any injury to people or property resulting from any ideas, methods, instructions or products referred to in the content.